Received: 19 March 2024 | Revised: 23 May 2024 | Accepted: 1 July 2024

DOI: 10.1002/jsp2.1358

RESEARCH ARTICLE

JOR Spine OPEN ACCESS

The morphological discrepancy of neuromuscular junctions between bilateral paraspinal muscles in patients with adolescent idiopathic scoliosis: A quantitative immunofluorescence assay

Tianyuan Zhang[1] | Wenyuan Sui[1] | Bin Li[1] | Xiexiang Shao[1] | Yaolong Deng[1] | Zifang Zhang[1] | Jingfan Yang[1] | Zifang Huang[2] | Wenjun Yang[1] | Junlin Yang[1,2]

[1]Spine Center, Department of Pediatric Orthopedics, Xinhua Hospital Affiliated to Shanghai Jiaotong University School of Medicine, Shanghai, China

[2]Department of Spine Surgery, The Third Affiliated Hospital of Sun Yat-sen University, Guangzhou, China

Correspondence
Wenjun Yang and Junlin Yang, Spine Center, Department of Pediatric Orthopedics, Xinhua Hospital Affiliated to Shanghai Jiao Tong University, School of Medicine, No.1665 Kongjiang Road, Shanghai 200092, China.
Email: wjyang@sibcb.ac.cn; yjunlin@126.com

Funding information
National Natural Science Foundation of China, Grant/Award Numbers: 82072519, 82272166

Abstract

Introduction: Prior studies suggested that neuromuscular factors might be involved in the pathogenesis of adolescent idiopathic scoliosis (AIS). The neuromuscular junction (NMJ) is the important pivot where the nervous system interacts with muscle fibers, but it has not been well characterized in the paraspinal muscles of AIS. This study aims to perform the quantitative morphological analysis of NMJs from paraspinal muscles of AIS.

Methods: AIS patients who received surgery in our center were prospectively enrolled. Meanwhile, age-matched congenital scoliosis (CS) and non-scoliosis patients were also included as controls. Fresh samples of paraspinal muscles were harvested intraoperatively. NMJs were immunolabeled using different antibodies to reveal presynaptic neuronal architecture and post-synaptic motor endplates. A confocal microscope was used to acquire z-stack projections of NMJs images. Then, NMJs images were analyzed on maximum intensity projections using ImageJ software. The morphology of NMJs was quantitatively measured by a standardized 'NMJ-morph' workflow. A total of 21 variables were measured and compared between different groups.

Results: A total of 15 AIS patients, 10 CS patients and 5 normal controls were enrolled initially. For AIS group, NMJs in the convex side of paraspinal muscles demonstrated obviously decreased overlap when compared with the concave side (34.27% ± 8.09% vs. 48.11% ± 10.31%, $p = 0.0036$). However, no variables showed statistical difference between both sides of paraspinal muscles in CS patients. In

Tianyuan Zhang and Wenyuan Sui contributed equally to this work and should be listed as co-first authors.

contrast with non-scoliosis controls, both sides of paraspinal muscles in AIS patients demonstrated significantly smaller muscle bundle diameters.

Conclusions: This study first elucidated the morphological features of NMJs from paraspinal muscles of AIS patients. The NMJs in the convex side showed smaller overlap for AIS patients, but no difference was found in CS. This proved further evidence that neuromuscular factors might contribute to the mechanisms of AIS and could be considered as a novel potential therapeutic target for the treatment of progressive AIS.

KEYWORDS

adolescent idiopathic scoliosis, immunofluorescence staining, morphological analysis, neuromuscular junctions, paraspinal muscles

1 | INTRODUCTION

Scoliosis refers to the lateral curvature of the spine of 10 degrees or more (the Cobb angle). Adolescent idiopathic scoliosis (AIS) is the most common form of structural spinal deformities and is different from other types of scoliosis that have underlying congenital or neuromuscular abnormalities.[1] AIS develops curves in healthy individuals without clear symptoms and its etiology still remains unknown.[2] Many hypotheses had been proposed, such as genetics, biomechanics, skeletal spinal growth, environmental factors and et al.[3] Nowadays, more and more researchers paid attention to the involvement of neuromuscular factors and regarded AIS as neuropathic or myopathic disorders.[4–7] For example, Blecher et al. used genetic mouse models to demonstrate the central role of proprioception in maintaining spinal alignment and they found that mutants for specific genes could develop scoliosis phenotype similar to AIS.[8] Wang et al. identified genetic variants of SLC6A9 in AIS, which led to the aberrant glycinergic neurotransmission, and slc6a9 mutant zebrafish exhibited discoordination of spinal neural activities and pronounced lateral spinal curvature, resembling human patients.[9] Shao et al. found the deficiency of ESR1 in muscle progenitor cells of paraspinal muscles for AIS patients and imbalance of ESR1 signaling in bilateral paraspinal muscles induced scoliosis in mice.[10] These clues supported that the neuromuscular factors might be closely involved in the pathogenesis of AIS, but the exact mechanism still remained to be elucidated.

Synapses, the fundamental units in neuronal circuits of nervous system, are critical for proper communications between neurons and between a neuron and its target cell.[11] The neuromuscular junctions (NMJs) are chemical synapses formed between motoneurons and skeletal muscle fibers and are essential for controlling muscle contraction. Improper formation and maintenance of NMJs are often observed in various neuromuscular disorders, such as Duchenne muscular dystrophy (DMD) and spinal muscular atrophy (SMA), representing an important approach to study pathogenetic alterations.[12–14]

On the other hand, these neuromuscular diseases developed secondary scoliosis much more frequently during the course of these pathologies than does "idiopathic" scoliosis in the general population: prevalence ranged from 25 to 100% according to etiology.[15] For example, Kinali et al. found that about 75%–90% patients with DMD would develop scoliosis.[16] Wijngaarde et al. observed that the lifetime probability of receiving scoliosis surgery was almost 80% in SMA type 1c and 2 patients.[17] Therefore, abnormal NMJs in the paraspinal muscles had close association with the onset of scoliosis for these neuromuscular disorders. And we wondered if such potential relationship existed for AIS patients. However, few studies had examined the morphological changes of NMJs from paraspinal muscles of AIS patients, although abnormal neuromuscular evidence had been detected as pointed out above. For the first time, this study performed the quantitative morphological analysis of NMJs from bilateral paraspinal muscles of AIS patients. We also collected samples from congenital scoliosis (CS) and non-scoliosis patients to make a comparison.

2 | MATERIALS AND METHODS

2.1 | Study participants

This was a prospective enrolled study. Institutional review board approval was obtained for the study (No. XHEC-D-2019-093). This study was performed according to the Declaration of Helsinki. All cases signed informed consent before their inclusion in the study. The inclusion criteria for AIS and CS patients were (1) 10 to 18 years old and (2) received posterior scoliosis correction surgery from August 2021 to August 2022 in our center. The inclusion criteria for non-scoliosis patients were (1) 10 to 18 years old and (2) received posterior spinal surgery due to vertebral fracture or lumbar disc herniation during the same period. Samples collected from non-scoliosis patients were regarded as normal controls. Participants who were reluctant to participate the study or declined to provide informed consent were excluded. All surgical procedures were performed by the same surgical team and about 200 cases were operated during this time. The whole-spine MRI was performed to exclude any intraspinal abnormity for AIS

patients. The baseline clinical and radiographic information were collected, including sex, age, height, weight and body mass index (BMI). The magnitude of scoliosis curve angle was measured by Cobb's method on the full-spine standing radiographs. The apical vertebral translation (AVT, distance between the plumb line and the center of the apical vertebra/disc) was also measured.

2.2 | Tissue sampling

For AIS and CS patients, muscle tissues were sampled intraoperatively from the bilateral deep paraspinal muscles in the apical region of main curves. For non-scoliosis patients, deep paraspinal muscles were also collected from the operated vertebral level in only one side. The long-stripe blocks of tissues (approx. 2 cm in length) were collected because we didn't know the exact location of NMJs in advance during sampling and too short muscle bundle often had no NMJs on it.[18] Immediately, muscle samples were fixed overnight in 4% paraformaldehyde (PFA) after drying in excess blood and removing visible fat/connective tissues. Then, samples were washed in phosphate-buffered saline (PBS) three times and stored in PBS until labeling.

2.3 | NMJs staining

To label NMJs, small bundles of 20–30 muscle fibers were first teased from the large whole muscles under a stereomicroscope. NMJs were immunohistochemically labeled using a standard laboratory protocol for visualizing pre- and post-synaptic apparatus[19]: 1. Transfer muscle bundles into 16-well plates containing 1% bovine serum albumin (BSA) and 0.5% Triton X-100 and keep them under gentle agitation for 1 h at room temperature (RT); 2. Wash samples 3 times for 5 min with PBS at RT; 3. Incubate samples with the primary antibodies in 5% BSA overnight at 4°C; 4. Wash samples 3 times for 5 min with PBS at RT; 5. Incubate samples with the secondary antibodies in 1% PBS overnight at 4°C; 6. Wash samples 3 times for 5 min with PBS at RT; 7. Place them on a slide with an antifade mounting medium (Aqua-Poly/Mount) and cover them with a cover slip; 8. Store at −20°C prior to imaging. The primary antibodies were rabbit anti-neurofilament-L (1:200, Cell Signaling Technology, #2837S) to label innervating axons and rabbit anti-synapsin-1 (1:400, Cell Signaling Technology, #5297S) to label presynaptic nerve terminals. The secondary antibodies were Alexa Fluor 488 goat anti-rabbit immunoglobin (1:500, Invitrogen, #A11034) and tetramethylrhodamine-conjugated α-bungarotoxin (α-BTX) (1:500, Invitrogen, #T1175) to label post-synaptic acetylcholine receptors (AChRs).

2.4 | Morphology analysis of NMJs

Confocal images were acquired and analyzed using a standardized "NMJ-morph" workflow.[20] Briefly, a Leica TCS SP8 confocal microscope was used to acquire z-stack projections of NMJs and their preterminal axon. We routinely used 10× objective to scan and locate the position of NMJs on muscle bundles. Then, 40× oil immersion objective was used to get the images of NMJs. Confocal settings were adjusted as follows to achieve high image quality: 8-bit depth, 512 × 512 frame size, 400 speed, system optimized z-stack interval, green channel (488 nm excitation, 500–550 nm collection), red channel (547 nm excitation, 565–615 nm collection). Images were then analyzed on maximum intensity projections of the z-stacks, using ImageJ software. The NMJ-morph workflow measured 21 separate morphological variables for each NMJ, including pre-synaptic variables (nerve terminal area, nerve terminal perimeter, number of terminal branches, number of branch points, total length of branches), post-synaptic variables (AChR area, AChR perimeter, endplate area, endplate perimeter, endplate diameter, number of AChR clusters), derived variables (average length branches, complexity, compactness, area of synaptic contact, overlap, average area AChR clusters, fragmentation) and related nerve and muscle measurements (axon diameter, muscle bundle diameter, number of axonal inputs). The basic pre- and post-synaptic variables were widespread used and easy to understand literally. Some of derived variables were explained as follows:

$$\textbf{Average length branches} = \text{total length of branches} \div \text{number of terminal branches}$$

$$\textbf{Area of synaptic contact} = \text{total area of AChRs} - \text{unoccupied area of AChRs}$$

$$\textbf{Complexity} = \log_{10}(\text{number of terminal branches} \times \text{number of branch points} \times \text{total length of branches})$$

$$\textbf{Compactness} = (\text{AChR area} \div \text{endplate area}) \times 100\%$$

$$\textbf{Overlap} = [(\text{total AChR area} - \text{unoccupied AChR area}) \div \text{total AChR area}] \times 100\%$$

$$\textbf{Fragmentation} = 1 - (1 \div \text{number of AChR clusters})$$

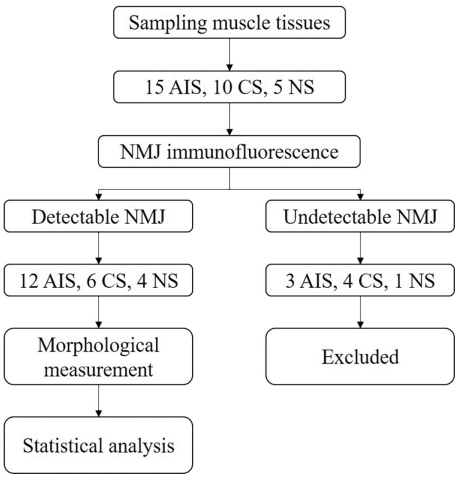

FIGURE 1 The flow chart of the study. (AIS = adolescent idiopathic scoliosis, CS = congenital scoliosis, NS = normal subjects, NMJ = neuromuscular junction).

TABLE 1 The baseline clinical information of different groups.

	AIS patients	CS patients	Controls	*p* value
Age (years)	13.58 ± 1.78	14.67 ± 2.16	14.50 ± 1.29	0.440
Sex				0.826
Male	3	2	2	
Female	9	4	2	
Height (cm)	155.17 ± 6.67	156.50 ± 7.97	158.75 ± 4.79	0.659
Weight (kg)	43.02 ± 7.20	46.67 ± 5.50	51.25 ± 8.54	0.142
BMI (kg/m^2)	17.73 ± 2.13	19.11 ± 2.24	20.25 ± 2.45	0.141
Main curve (°)	63.58 ± 12.50	62.50 ± 7.58	-	0.849
AVT (mm)	44.00 ± 18.03	48.33 ± 8.16	-	0.587

Abbreviations: AIS, adolescent idiopathic scoliosis; AVT, apical vertebra translation; BMI, body mass index; CS, congenital scoliosis.

TABLE 2 Overview of NMJs' morphological variables.

	AIS concave	AIS convex	CS concave	CS convex	Normal Subjects	*p* value
Core variables						
Pre-synaptic						
Nerve Terminal Perimeter (μm)	72.84 ± 20.99	65.34 ± 15.63	82.75 ± 26.95	76.89 ± 8.843	88.06 ± 28.35	0.38
Nerve Terminal Area (μm^2)	100.90 ± 77.59	64.11 ± 14.42	103.76 ± 63.79	95.68 ± 27.55	113.91 ± 73.05	0.49
Number of Terminal Branches	7.23 ± 4.99	7.41 ± 4.32	9.15 ± 3.63	12.1 ± 5.30	8.19 ± 0.93	0.52
Number of Branch Points	2.86 ± 2.53	2.71 ± 3.59	3.42 ± 2.37	5.88 ± 3.94	3.57 ± 1.36	0.59
Total Length of Branches (μm)	32.95 ± 16.14	29.00 ± 12.20	34.75 ± 12.72	34.88 ± 7.801	38.64 ± 14.84	0.82
Post-synaptic						
AChR Perimeter (μm)	107.57 ± 51.07	112.08 ± 50.34	113.84 ± 27.14	111.90 ± 33.48	100.24 ± 36.02	0.99
AChR Area (μm^2)	128.90 ± 36.07	154.98 ± 37.40	147.55 ± 43.41	123.92 ± 7.19	145.39 ± 79.16	0.54
Endplate Diameter (μm)	23.79 ± 3.68	24.87 ± 2.74	30.18 ± 10.44	27.08 ± 3.92	24.87 ± 8.33	0.34
Endplate Perimeter (μm)	68.81 ± 9.44	71.70 ± 10.62	82.23 ± 18.51	70.26 ± 7.26	68.73 ± 21.90	0.48
Endplate Area (μm^2)	249.75 ± 67.64	274.91 ± 63.03	315.50 ± 97.90	238.55 ± 32.61	279.93 ± 162.60	0.66
Number of AChR Clusters	3.45 ± 2.09	3.30 ± 2.05	2.97 ± 0.33	3.25 ± 1.47	3.40 ± 0.66	0.99
Derived variables						
Pre-synaptic						
Average Length of Branches (μm)	4.85 ± 1.44	4.44 ± 1.46	5.91 ± 1.86	4.70 ± 1.26	5.30 ± 2.04	0.57
Complexity	2.64 ± 0.92	2.51 ± 0.82	2.57 ± 0.48	2.80 ± 0.31	2.78 ± 0.24	0.90
Post-synaptic						
Average Area of AChR Clusters (μm^2)	55.79 ± 23.11	68.45 ± 21.36	66.09 ± 31.57	52.73 ± 19.31	53.08 ± 27.88	0.62
Fragmentation	0.52 ± 0.22	0.52 ± 0.16	0.57 ± 0.09	0.58 ± 0.16	0.59 ± 0.03	0.93
Compactness (%)	52.52 ± 6.22	55.76 ± 812	50.98 ± 4.62	54.28 ± 4.37	52.98 ± 6.03	0.55
Overlap (%)	48.11 ± 10.31	34.27 ± 8.09	43.23 ± 13.28	43.34 ± 19.40	53.87 ± 9.27	0.03*
Area of Synaptic Contact (μm^2)	57.14 ± 18.11	49.84 ± 12.27	70.22 ± 44.30	50.05 ± 14.87	79.24 ± 48.21	0.32
Associated nerve and muscle variables						
Axon Diameter (μm)	1.68 ± 0.51	1.68 ± 0.38	2.01 ± 0.20	1.79 ± 0.067	1.83 ± 0.88	0.77
Number of Axonal Inputs	1.02 ± 0.04	1.02 ± 0.04	1.00 ± 0.00	1.04 ± 0.07	1.03 ± 0.05	0.75
Muscle Bundle Diameter (μm)	49.71 ± 15.99	55.35 ± 21.49	57.50 ± 16.49	57.99 ± 15.76	82.35 ± 18.28	<0.0001*

Note: One-way ANOVA is used here to compare different groups, *means significantly different.
Abbreviations: AIS, adolescent idiopathic scoliosis; CS, congenital scoliosis; NMJ, neuromuscular junction.

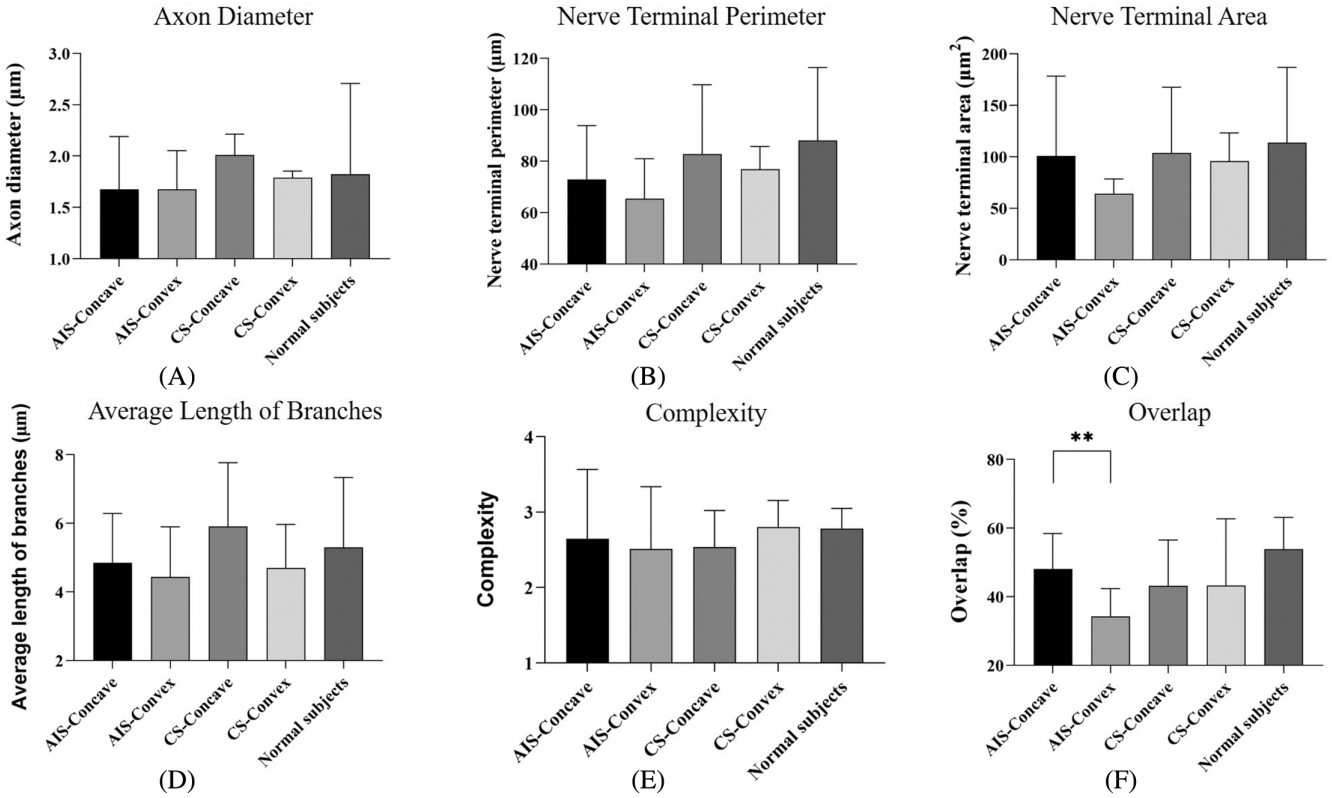

FIGURE 2 Diagrams of pre-synaptic associated variables. (A) axon diameter; (B) nerve terminal perimeter; (C) nerve terminal area; (D) average length of branches; (E) complexity; (F) overlap. (AIS = adolescent idiopathic scoliosis, CS = congenital scoliosis, *means significantly different).

On average, approximately 25–30 NMJs were measured for each sample. The researcher who performed the measurements was blinded to the clinical information.

2.5 | Statistical analysis

Data were presented as mean ± standard deviation. Statistical analysis was performed by GraphPad Prism 9 (GraphPad Software Inc., San Diego, CA, USA). The paired *t*-test was used between both sides of paraspinal muscles in AIS and CS, and one-way analysis of variance (ANOVA) was used among three groups. Difference was considered significant with $p < 0.05$.

3 | RESULTS

3.1 | Cohorts

A total of 30 patients, including 15 AIS patients, 10 CS patients and 5 normal subjects, were prospectively sampled in this study initially. After immunolabeling, we confirmed the locations of NMJs in paraspinal muscles and some cases were excluded due to no detection of NMJs. Finally, 22 patients, including 12 AIS, 6 CS and 4 normal subjects, were included in the subsequent analysis. The flow chart of this study is shown in Figure 1. The age, sex, height, weight and BMI showed no statistical difference among three groups (Table 1). The Cobb angel of the main curve and AVT also showed no significant difference between AIS and CS patients. The NMJs were imaged and analyzed for both sides of paraspinal muscles in AIS patients. The two sides in CS patients were also compared, aiming at investigating the potential changes of NMJs secondary to the onset of scoliosis.

3.2 | NMJs analysis

Qualitatively, rough observations revealed that NMJs of paraspinal muscles in AIS patients had "nummular" morphological feature, similar to the normal appearance of human NMJs. We did not observe evidence of gross pathological changes, such as denervation or fragmented endplates. Then, we performed the comprehensive morphological analysis to investigate the microscopic subtle changes of NMJs between both sides of paraspinal muscles. A total of 21 variables were measured for each NMJ, and the overview of NMJs' morphological variables is shown in Table 2.

For pre-synaptic part, few axonal spread-out or multiple innervation were found. The axon diameter showed no difference between both sides of paraspinal muscles. The convex side of paraspinal muscles had decreased nerve terminal perimeter, nerve terminal area,

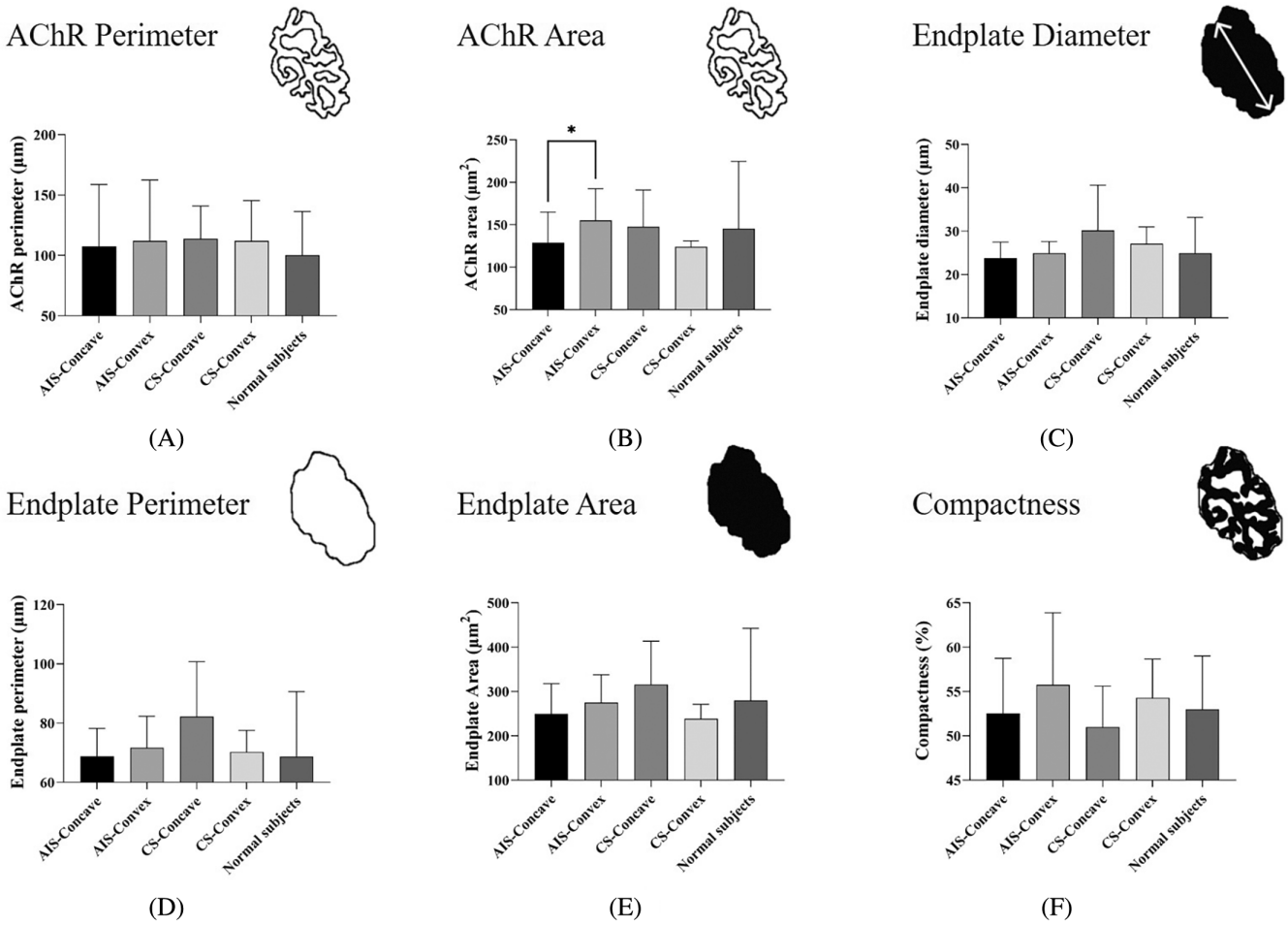

FIGURE 3 Diagrams of post-synaptic associated variables. (A) AChR perimeter; (B) AChR area; (C) endplate diameter; (D) endplate perimeter; (E) endplate area; (F) compactness. (AChR = acetylcholine receptor, AIS = adolescent idiopathic scoliosis, CS = congenital scoliosis, *means significantly different).

average length of branches and complexity when compared with the concave side, but no statistical significance was reached (Figure 2). For post-synaptic variables, NMJs in the concave side of paraspinal muscles had significantly smaller AChR area, but no significant difference was noted among three groups (Table 2. $p = 0.54$). Other post-synaptic variables also showed no obvious difference (Figure 3).

Strikingly, we found that NMJs in the convex side of paraspinal muscles had significantly decreased overlap when compared with the concave side, which described the percentage of congruence between the pre- and post-synaptic elements of the NMJ—the extent to which the nerve terminal matched the AChR (Figure 2, $p = 0.0036$). However, the overlap of NMJs in CS patients demonstrated no significant difference between both sides. The overlap of NMJs in the convex paraspinal muscles of AIS was also significantly smaller than that in normal controls (Figure 4). Correlation analysis was then performed between overlap difference and clinical data in AIS, but no statistical significance was found (Table 3).

Regarding to related nerve and muscle variables, we found that the mean muscle bundle diameter in the convex side of AIS was slightly larger than the concave side (Figure 5, $p = 0.0005$). However, when compared with normal controls, the mean diameter of muscle bundle was significantly smaller in both sides of AIS and CS patients (Figure 5, all $p < 0.0001$).

4 | DISCUSSION

Despite decades of research, the primary cause of AIS still remained uncertain and many arguments existed.[21,22] Among them, paraspinal muscular abnormities and neurological deficits played important roles, but how these factors drive scoliosis and interplay with each other were complicated and perplexing.[23] The NMJ was a peripheral synapse between motoneurons and skeletal muscle fibers that was critical to control muscle contractions. Dysfunction of NMJs could destroy the intimate interaction between motor nerve terminals and muscle fibers, finally causing neuromuscular dysfunction. Thus, diseases of NMJs in the paravertebral muscles would easily influence the spinal stability and balance. For example, for patients with scoliosis associated with syringomyelia, Zhu et al. found there were abnormal diffusion of AChRs at extra-junctional sites and the existence of immature gamma-AChR

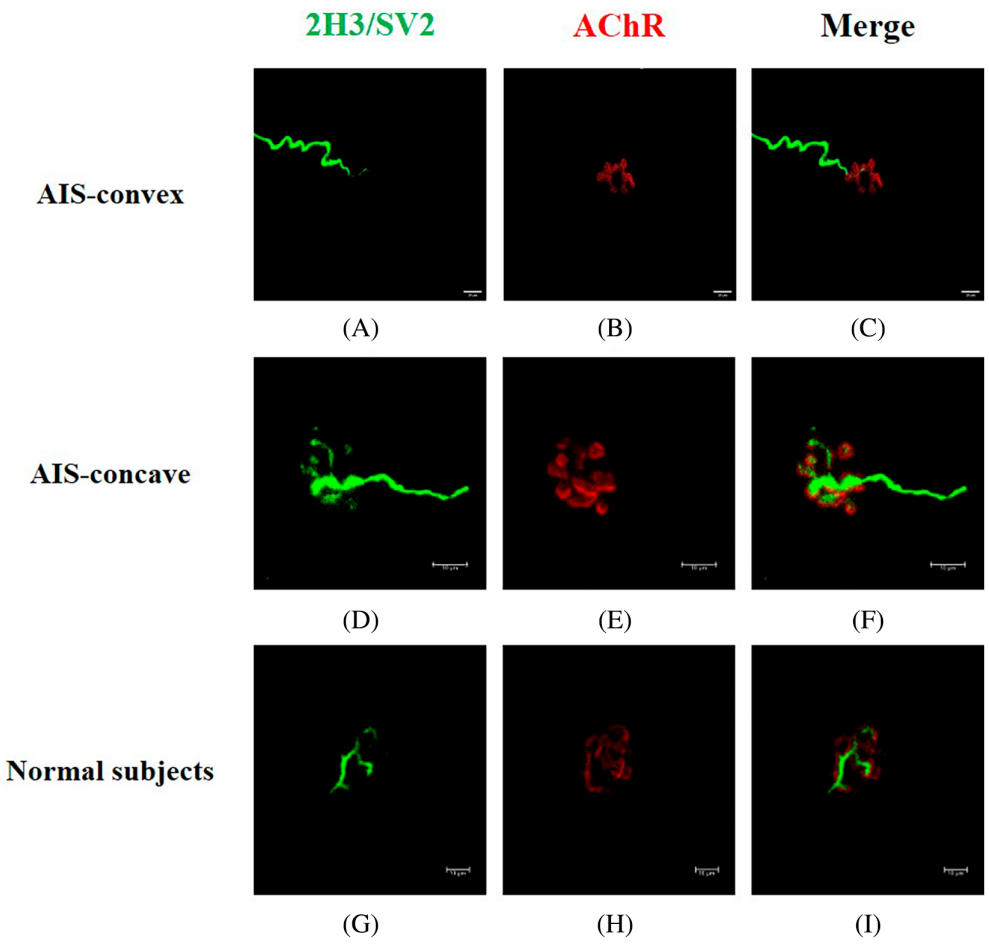

FIGURE 4 Examples of neuromuscular junctions of paraspinal muscles. (A–C) the convex side of AIS; (D–F) the concave side of AIS; (G–I) normal subjects. (AIS = adolescent idiopathic scoliosis, 2H3 = neurofilament, SV2 = synaptic vesicle, AChR = acetylcholine receptor).

TABLE 3 The correlation analysis between overlap difference and clinical data in AIS.

		Age	Sex	Height	Weight	BMI	Cobb angle	AVT
Overlap difference	*r*	−0.220	0.412	−0.082	0.028	0.147	−0.280	−0.095
	p	0.601	0.310	0.847	0.948	0.729	0.501	0.822

Note: Overlap difference was defined as subtracting overlap in the convex side from overlap in the concave side.
Abbreviations: AIS, adolescent idiopathic scoliosis, AVT, apical vertebra translation; BMI = body mass index.

subunit in the paravertebral muscles.[24] Besides, Theroux et al. also reported that there was an abnormal distribution of AChRs relative to the acetylcholinesterase found at the NMJs of paravertebral muscles in patients with cerebral palsy and concomitant scoliosis.[25] However, no studies had thoroughly explored weather there were morphological abnormalities of NMJs in paravertebral muscles for AIS patients. Recently, more and more researches supported the evidence of neuromuscular pathogenic factors for AIS. Therefore, we speculated that the NMJs of paravertebral muscles may be affected to some extent in AIS. To solve this problem, we carried out this quantitative immunofluorescence assay to compare the morphology of NMJs between both sides of paravertebral muscles in AIS patients.

Importantly, this study revealed that NMJs in the convex side of paravertebral muscles from AIS patients had significantly lower overlap when compared with the concave side. On the other words, the degree of congruence that nerve terminal matched the AChR was less in the convex side. This finding meant that paraspinal muscles in the convex side might have the phenomenon of neurogenic abnormities, thus causing dysfunction of neuromuscular systems. In this way, we hypothesized that bilateral paraspinal muscles had asymmetric capability of neuromuscular transmission and muscle contraction at the onset, thereby driving the formation of scoliosis. We also investigated the potential correlation between overlap difference and clinical data, but no such relationship was found. Due to the relatively small sample sizes, the consequential lack of significance should be considered in this context with caution.

Consistent with our results, Liu et al. evaluated the biomechanical features of paravertebral muscles in AIS and found that muscle tone and stiffness on the concave side was significantly greater than that on the convex side.[26] Besides, the asymmetric biomechanical characteristics of paravertebral muscles were closely related to the severity of scoliosis. However, previous studies that focused on the

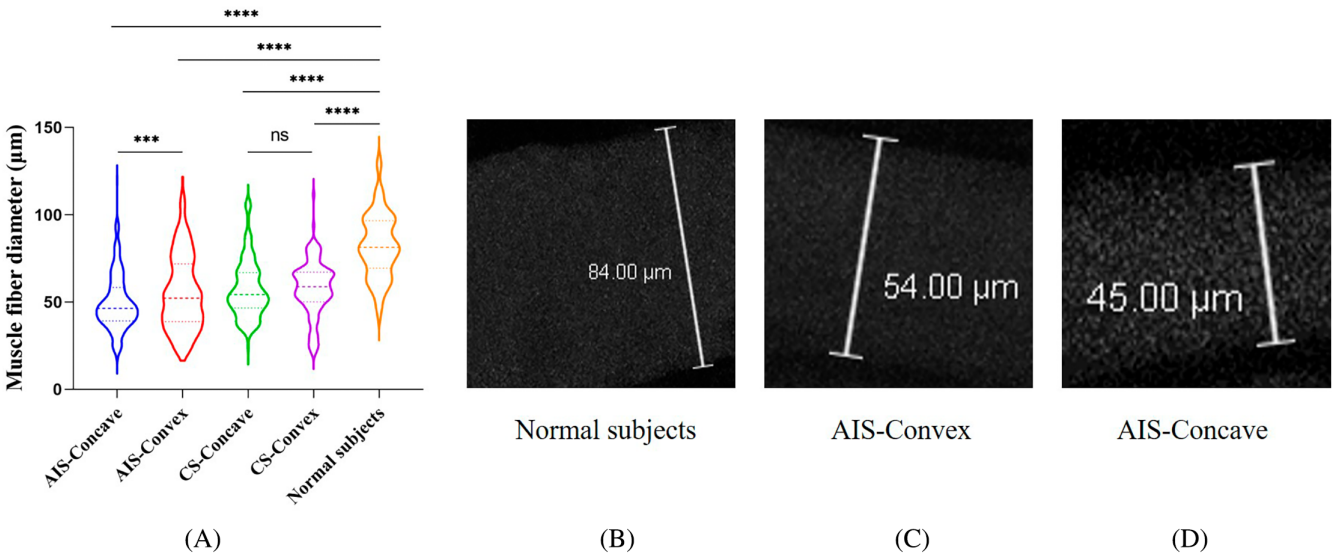

FIGURE 5 Schematic diagrams of muscle bundle diameter. (A) Violin plot of muscle bundle diameter from different groups. (B) Example of muscle bundle diameter from normal subjects; (C) example from the convex side of paraspinal muscles in AIS; (D) example from the concave side of paraspinal muscles in AIS. (AIS = adolescent idiopathic scoliosis, *means significantly different).

asymmetry of spinal neuromuscular function by surface electromyogram (EMG) didn't reach a consensus. A recent review screened 94 related studies and summarized that for EMG amplitude, 43 outcome measures provided evidence of convex>concave activation, 85 outcomes supported no difference between sides, and 8 outcomes supported concave>convex activation.[27] Therefore, more precise experiments are needed to delineate the asymmetrical neuromuscular activity from paraspinal muscles of AIS patients in the future. This article first provided evidence from the morphological view, but how it affected the functional alterations still remained to be explored.

It was known that the structure of NMJs generally remained stable in young, healthy populations with life-long maintenance after its maturation. However, evidence existed that there was a significant degree of structural plasticity at this synapse, which meant NMJs underwent a subtle form of remodeling continuously responding to different circumstances.[28] For example, the morphological and physiological variability of the NMJs had been shown to adapt to both increased and decreased use of muscle tissues.[29] Therefore, we had to evaluate whether the morphological changes of NMJs from paraspinal muscles of AIS patients were primary disorders, or secondary to the onset of scoliosis curve. To solve this problem, age- and curve-matched CS patients were also recruited and analyzed in this study. Our results revealed that the morphological overlap difference of NMJs between both sides of paraspinal muscles in AIS might be a primary cause driving the onset of scoliosis and provided further evidence that neuromuscular deficits were closely involved in the pathogenesis of AIS.

This study had several limitations. First, this study came from one single center and the sample size was relatively small. Second, potential measurement errors still existed despite following the standardized workflow. Third, this study only focused on the morphological analysis, but did not explore the gene expression profiles of NMJs. Actually, The majority of muscle samples were not synaptic, and would cover the expression of NMJ-specific genes, since NMJs region represented only 0.01%–0.1% of muscle fibers.[30] Therefore, it was difficult to characterize the molecular profiles of NMJs without extracting the NMJ-specific regions from the whole-mount muscles. Fourth, the diameter of muscle bundle was measured based on the longitudinal plane. It had the inherent limitation that the measuring location which was differently chosen would influence the results, although we usually measured muscle bundles without obvious folds or curves. Finally, this study did not explain the functional alterations of neuromuscular activities in AIS patients. More accurate methods were needed to investigate the functions of paraspinal muscles in the future.

5 | CONCLUSIONS

The present study elucidated the morphological features of NMJs from bilateral paraspinal muscles of AIS patients and made a comparison with CS and non-scoliosis patients. Our results demonstrated the decreased overlap in the convex side of paraspinal muscles exclusively for AIS patients, but no such disorder of NMJs existed in CS patients. This indicated that NMJs' abnormities were not derived from the consequence of scoliosis and neuromuscular factors might contribute to the mechanisms of AIS. Besides, it could be considered as a novel potential therapeutic target for the treatment of progressive AIS.

AUTHOR CONTRIBUTIONS

JLY, and WJY conceived and designed the study; TYZ, BL, WYS, and XXS performed the experiments and analyzed the data; TYZ, and WYS drafted the manuscript; YLD, ZFZ, JFY, and ZFH revised the

manuscript. All authors have approved the final version of the manuscript and have agreed to be accountable for all aspects of the work.

ACKNOWLEDGMENTS

We thank the staff members of the Integrated Laser Microscopy System at the National Facility for Protein Science in Shanghai (NFPS), Shanghai Advanced Research Institute, Chinese Academy of Sciences, China for sample preparation, data collection and analysis.

FUNDING INFORMATION

This work was supported by the National Nature Science Foundation of China (82272166, 82072519).

CONFLICT OF INTEREST STATEMENT

The authors declare that they have no competing financial interest.

ORCID

Bin Li https://orcid.org/0000-0003-4521-8989
Junlin Yang https://orcid.org/0000-0001-9809-1219

REFERENCES

1. Kuznia AL, Hernandez AK, Lee LU. Adolescent idiopathic scoliosis: common questions and answers. *Am Fam Physician*. 2020;101(1):19-23.
2. Altaf F, Gibson A, Dannawi Z, Noordeen H. Adolescent idiopathic scoliosis. *BMJ*. 2013;346:f2508.
3. Cheng JC, Castelein RM, Chu WC, et al. Adolescent idiopathic scoliosis. *Nat Rev Dis Primers*. 2015;1:15030.
4. Faloon M, Sahai N, Pierce TP, et al. Incidence of neuraxial abnormalities is approximately 8% among patients with adolescent idiopathic scoliosis: a meta-analysis. *Clin Orthop Relat Res*. 2018;476(7):1506-1513.
5. Veldhuizen AG, Wever DJ, Webb PJ. The aetiology of idiopathic scoliosis: biomechanical and neuromuscular factors. *Eur Spine J*. 2000;9(3):178-184.
6. Deng M, Hui SC, Yu FW, et al. MRI-based morphological evidence of spinal cord tethering predicts curve progression in adolescent idiopathic scoliosis. *Spine J*. 2015;15(6):1391-1401.
7. Chu WC, Lam WW, Chan YL, et al. Relative shortening and functional tethering of spinal cord in adolescent idiopathic scoliosis?: study with multiplanar reformat magnetic resonance imaging and somatosensory evoked potential. *Spine (Phila Pa 1976)*. 2006;31(1):E19-E25.
8. Blecher R, Krief S, Galili T, et al. The proprioceptive system masterminds spinal alignment: insight into the mechanism of scoliosis. *Dev Cell*. 2017;42(4):388-399.e3.
9. Wang X, Yue M, Cheung JPY, et al. Impaired glycine neurotransmission causes adolescent idiopathic scoliosis. *J Clin Invest*. 2024;134(2):e168783.
10. Shao X, Fu X, Yang J, et al. The asymmetrical ESR1 signaling in muscle progenitor cells determines the progression of adolescent idiopathic scoliosis. *Cell Discov*. 2023;9(1):44.
11. Li L, Xiong WC, Mei L. Neuromuscular junction formation, aging, and disorders. *Annu Rev Physiol*. 2018;80:159-188.
12. Qaisar R. Targeting neuromuscular junction to treat neuromuscular disorders. *Life Sci*. 2023;333:122186.
13. Arnold WD, Clark BC. Neuromuscular junction transmission failure in aging and sarcopenia: the nexus of the neurological and muscular systems. *Ageing Res Rev*. 2023;89:101966.
14. Ng SY, Ljubicic V. Recent insights into neuromuscular junction biology in Duchenne muscular dystrophy: impacts, challenges, and opportunities. *EBioMedicine*. 2020;61:103032.
15. Vialle R, Thévenin-Lemoine C, Mary P. Neuromuscular scoliosis. *Orthop Traumatol Surg Res*. 2013;99(1 Suppl):S124-S139.
16. Kinali M, Messina S, Mercuri E, et al. Management of scoliosis in Duchenne muscular dystrophy: a large 10-year retrospective study. *Dev Med Child Neurol*. 2006;48(6):513-518.
17. Wijngaarde CA, Brink RC, de Kort FAS, et al. Natural course of scoliosis and lifetime risk of scoliosis surgery in spinal muscular atrophy. *Neurology*. 2019;93(2):e149-e158.
18. Jones RA, Harrison C, Eaton SL, et al. Cellular and molecular anatomy of the human neuromuscular junction. *Cell Rep*. 2017;21(9):2348-2356.
19. Boehm I, Miller J, Wishart TM, et al. Neuromuscular junctions are stable in patients with cancer cachexia. *J Clin Invest*. 2020;130(3):1461-1465.
20. Jones RA, Reich CD, Dissanayake KN, et al. NMJ-morph reveals principal components of synaptic morphology influencing structure-function relationships at the neuromuscular junction. *Open Biol*. 2016;6(12):160240.
21. Zaina F, Wynne J, Cohen L. Scoliosis and spinal deformities: twenty years of innovations. *Eur J Phys Rehabil Med*. 2023;59(4):502-504.
22. Sun D, Ding Z, Hai Y, Cheng Y. Advances in epigenetic research of adolescent idiopathic scoliosis and congenital scoliosis. *Front Genet*. 2023;14:1211376.
23. Kiram A, Hu Z, Man GC, et al. The role of paraspinal muscle degeneration in coronal imbalance in patients with degenerative scoliosis. *Quant Imaging Med Surg*. 2022;12(11):5101-5113.
24. Zhu Z, Qiu Y, Wang B, Yu Y, Qian B, Zhu F. Abnormal spreading and subunit expression of junctional acetylcholine receptors of paraspinal muscles in scoliosis associated with syringomyelia. *Spine (Phila Pa 1976)*. 2007;32(22):2449-2454.
25. Theroux MC, Akins RE, Barone C, Boyce B, Miller F, Dabney KW. Neuromuscular junctions in cerebral palsy: presence of extrajunctional acetylcholine receptors. *Anesthesiology*. 2002;96(2):330-335.
26. Liu Y, Pan A, Hai Y, Li W, Yin L, Guo R. Asymmetric biomechanical characteristics of the paravertebral muscle in adolescent idiopathic scoliosis. *Clin Biomech (Bristol, Avon)*. 2019;65:81-86.
27. Ng PTT, Claus A, Izatt MT, Pivonka P, Tucker K. Is spinal neuromuscular function asymmetrical in adolescents with idiopathic scoliosis compared to those without scoliosis?: a narrative review of surface EMG studies. *J Electromyogr Kinesiol*. 2022;63:102640.
28. Rodríguez Cruz PM, Cossins J, Beeson D, Vincent A. The neuromuscular junction in health and disease: molecular mechanisms governing synaptic formation and homeostasis. *Front Mol Neurosci*. 2020;13:610964.
29. Wilson MH, Deschenes MR. The neuromuscular junction: anatomical features and adaptations to various forms of increased, or decreased neuromuscular activity. *Int J Neurosci*. 2005;115(6):803-828.
30. Hui T, Jing H, Lai X. Neuromuscular junction-specific genes screening by deep RNA-seq analysis. *Cell Biosci*. 2021;11(1):81.

How to cite this article: Zhang T, Sui W, Li B, et al. The morphological discrepancy of neuromuscular junctions between bilateral paraspinal muscles in patients with adolescent idiopathic scoliosis: A quantitative immunofluorescence assay. *JOR Spine*. 2024;7(3):e1358. doi:10.1002/jsp2.1358